ISSN 0016-7029, Geochemistry International, 2016, Vol. 54, No. 5, pp. 423–438. © Pleiades Publishing, Ltd., 2016.

Geochemistry of Major and Rare Earth Elements in Garnet of the Kal-e Kafi Skarn, Anarak Area, Central Iran: Constraints on Processes in a Hydrothermal System[1]

S. Ranjbar[a], S. M. Tabatabaei Manesh[a,*], M. A. Mackizadeh[a], S. H. Tabatabaei[b], and O. V. Parfenova[c]

[a] *Department of Geology, Faculty of Science, University of Isfahan, Isfahan, Iran*

[b] *Department of Mining Engineering, Isfahan University of Technology, Isfahan, Iran*

[c] *Department of Petrology, Moscow State University, Lenincki Ave, 119991, Moscow, Russia*

******e-mail: tabatabalimp@gmail.com*

Received January 20, 2015; in final form, September 24, 2015

Abstract—Grossular-andradite (grandite) garnets, precipitated from hydrothermal solutions is associated with contact metamorphism in the Kal-e Kafi skarn show complex oscillatory chemical zonation. These skarn garnets preserve the records of the temporal evolution of contact metasomatism. According to microscopic studies and microprobe analysis profiles, the studied garnet has two distinct parts: the intermediate (granditic) composition birefringent core that its andradite content based on microprobe analysis varies between 0.68–0.7. This part is superimposed with more andraditic composition, and the isotropic rim which its andradite content regarding microprobe analysis ranges between 0.83–0.99. Garnets in the studied sample are small (0.5–2 mm in diameter) and show complex oscillatory zoning. Electron microprobe analyses of the oscillatory zoning in grandite garnet of the Kal-e Kafi area showed a fluctuation in chemical composition. The grandite garnets normally display core with intermediate composition with oscillatory Fe-rich zones at the rim. Detailed study of oscillatory zoning in grandite garnet from Kal-e Kafi area suggests that the garnet has developed during early metasomatism involving monzonite to monzodiorite granitoid body intrusion into the Anarak schist- marble interlayers. During this metasomatic event, Al, Fe, and Si in the fluid have reacted with Ca in carbonate rocks to form grandite garnet. The first step of garnet growth has been coeval with intrusion of the Kal-e Kafi granitoid into the Anarak schist- marble interlayers. In this period of garnet growth, change in fluid composition may cause the garnet to stop growing temporarily or keep growing but in a much slower rate allowing Al to precipitate rather than Fe. The next step consists of pervasive infiltration of Fe rich fluids and Fe rich grandite garnets formation as the rim of previously formed more Al rich garnets. Oscillatory zoning in the garnet probably reflects an oscillatory change in the fluid composition which may be internally and/or externally controlled. The rare earth elements study of these garnets revealed enrichment in light REEs (LREE) with a maximum at Pr and Nd and a negative to no Eu anomaly. This pattern is resulted from the uptake of REE out of hydrothermal fluids by growing crystals of calcsilicate minerals principally andradite with amounts of LREE controlled by the difference in ionic radius between Ca^{++} and REE^{3+} in garnet x site.

Keywords: Oscillatory zoning, Grandite garnets, Rare earth elements, Hydrothermal system, Kal-e Kafi, Iran

DOI: 10.1134/S0016702916050098

INTRODUCTION

Oscillatory zoning in minerals is a common phenomenon often formed by interacting with a fluid phase or melt (Shore and Fowler, 1996). In particular, the study of such zoning is a powerful tool for identifying the nature, source, and the evolution of fluids during contact metamorphism, specifically the genesis of skarn-type ore deposits (Clechenko and Walley, 2003).

Grossular-Andradite (grandite) garnets with oscillatory zoning are common in shallow contact metamorphic aureoles. Such garnets often display sharp micron-scale boundaries between zones, as well as very fine micrometer-scale zoning patterns (e.g., Lessing and Standish, 1973; Murad, 1976; Taylor and O'Neil, 1977; Hirai et al., 1982; Hirai and Nakazawa, 1982, 1986a, b; Akizuki et al., 1984; Jamtveit, 1991; Jamtveit et al., 1993, 1995; Jamtveit and Hervig, 1994; Ivanova et al., 1998; Smith et al., 2004; Gaspar et al., 2008).

Chemical zoning in grandites is mainly concerned with Fe^{3+}/A1 ratios but the distribution of minor and trace elements (for instance, Ti, As, Mn) can also be inhomogeneous (Jamtveit et al., 1995). Besides, $A1/Fe^{3+}$ ordering may result in the zonality which is visible with a polarizing microscope due to the degree

[1] The article is published in the original.

of birefringence or the orientation of the optical axes of extinction between the zones.

The rare-earth elements (REE) are widely used to model the petrogenesis and the evolution of igneous, sedimentary, and metamorphic rocks (e.g., see the summary by Haskin, 1984; Fleet, 1984). The REE are commonly regarded as being insensitive to all but the most intense hydrothermal processes. However, the literature supporting the mobility of REEs during hydrothermal processes has been increased in recent years (Nesbitt, 1979; Alderton et al., 1980; Humpheris, 1984; Marsh, 1991; Gouveia et al., 1993; Mongelli, 1993; Prndencio et al., 1993; Van der Weijden and Van der Weijden, 1995; Whitney and Olmsted, 1998). Recently, the potential of REE to provide information about ore forming processes has been properly recognized and detailed. REE investigations have been performed on many metallic deposits (Taylor and Fryer, 1980, 1982; Campbell et al., 1984; Giere, 1986; Whifford et al., 1988; Lottermoser, 1992; Parr, 1992; Wood and Williams-Jones, 1994; Bierlein, 1995; Bao and Zhao, 2003; Gaspar et al., 2008).

The studied area is in the vicinity of the Upper Eocene–Oligocene Kal-e Kafi granitoid body that is a part of Central East Iranian Micro-continent (CEIM). The studied skarn is located in 60 km northeast of Anarak and approximately 220 km northeast of Isfahan, Iran. Intrusion of this body into the Anarak schist-marble interlayers resulted in contact metamorphism and formation of skarn and hornfels (Fig. 1). Calcic garnets (grandites) in the skarn rocks show oscillatory zoning and in some instances, dodecahedral twins.

In this study, the results of complex zoning pattern investigation in samples from the Kal-e Kafi skarn, applying optical microscopy, scanning electron microscopy (SEM), electron probe microanalysis (EPMA), and the 2d element distribution maps for Fe, Mn, Ca and Mg are reported. The REE behavior in garnet from the skarn analyzed by the LA-ICP-MS method that is a powerful tool to constrain hydrothermal system evolution. The main purpose of this study is to present the detailed results of mineral chemistry and to discuss the observed pattern of major oxides and REEs in garnet.

GEOLOGICAL SETTING

The Kal-e Kafi granitoid is located in 60 km northeast of Anarak. It is a part of the Central Iranian Plateau and Yazd block. Ykovenko et al. (1981) in their regional prospect in this area included Kal-e Kafi as a part of Anarak- Khur massif. The most ancient rocks are represented by Anarak metamorphites (Chah Gorbeh and Derakhtak Schists) dated as upper Proterozoic. They are unconformably overlain by the Cretaceous terrigenous- carbonate rocks.

Volcanic series of the Eocene volcano- plutonic complex with a moderate level of acid composition rest on the Creaceous and rarely upper Protrozoic formations. The Kal-e Kafi intrusion has been resulted from the Alpine tectonomagmatic activities (Perfiliev et al., 1979).

Emplacement of the Kal-e Kafi intrusive body has been occurred in two stages. The first stage produced a medium and coarse grained granite, granosyenite, syenite, and monzonite (60 Ma, whole rock K-Ar (Perfiliev et al., 1979)). The second stage was noted for the appearance of equigranular and fine grained granite porphyries (53 Ma, whole rock K-Ar, (Perfiliv et al, 1979)) and also ring dykes. The reliability of the K-Ar ages is, however, debatable (Ahmadian et al, 2009). The monzonite- quarz monzonite and syenite are the most abundant rock types in contact with the Kal-e Kafi skarn. These intrusive rocks have been intruded into the upper Protrozoic schist and the marble interlayers. The Kal-e Kafi skarn occurs as exoskarn; whereas, endoskarn has not outcropped in the studied area.

ANALYTICAL METHODS

Samples were prepared from the polished thin sections, and then examined by petrographic microscope to define all patterns of zonation. Electron microprobe imaging and quantitative analysis were performed to determine the concentrations of F, Na, Mg, Al, Si, K, Ca, Ti, Cr, Mn, Fe and Ba using a Cameca SX-100 EMP at Stuttgart University, Germany, equipped with 5 wavelength-dispersive spectrometers. Counting times were 20 s at the peak. The applied acceleration voltage and electric current were 15 kV and 30 nA, respectively for analyzing garnet. Analytical errors of the applied method were reported by Massonne (2012). A number of minerals were analyzed on a JEOLEMP (JXA-8800) microscope with a wavelength-dispersive (WD) system at the Moscow State University, Russia. Element concentration maps for the major elements were prepared through a stepwise movement of thin section under electron beam of the microprobe and the subsequent computer aided evaluation (XMAP program, Bernhardt et al., 1995). Counting times per step were 100 ms an electric current of 40 nA was applied for scanning areas with garnet. For the calculation of structural formula of minerals and the content of molar fractions of mineral components from EMP analyses, the Excel Spread Sheet (garnet formula unit and endmember calculator) was utilized. In this program, garnet formula was calculated on the basis of 12 oxygene with Fe^{2+} and Fe^{3+} values recalculated following Droop method (1987). Structural statistics of pyroxene minerals were carried out by Minpet software.

Laser ablation (LA) was performed at a wavelength of 213 nm with a Cetac LSX 213 system coupled to the aforementioned ICP-MS in order to analyze garnet in

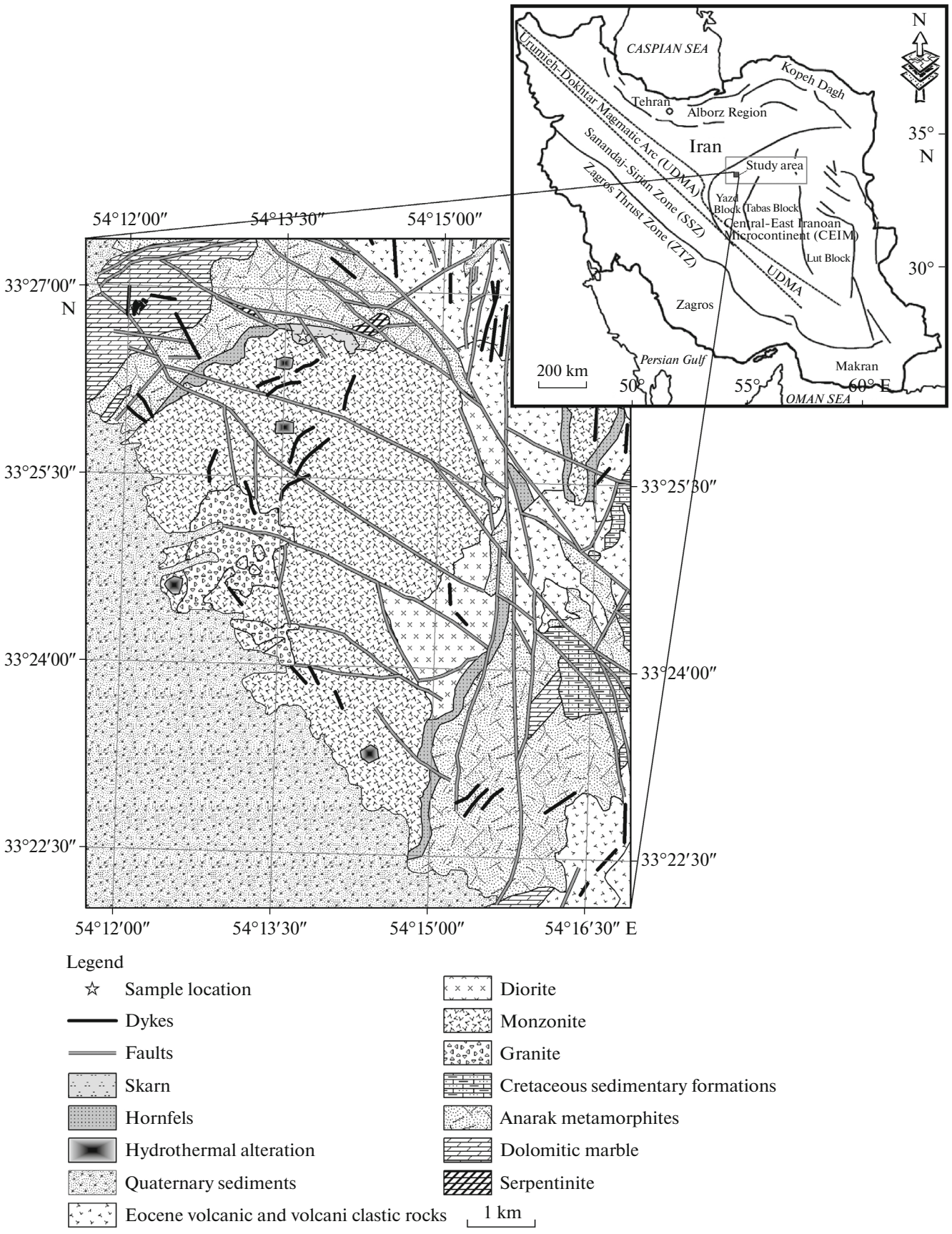

Fig. 1. Simplified geological map of the study area (after Technoexport, 1984).

a polished thin-section with a thickness of approximately 150 μm in Stuttgart University. Ablation diameters between 40 and 50 μm were selected and the incident laser energy was adjusted to 5% of its maximum. Ablation was performed at a pulse frequency of 20 Hz. The following multi-element standards were used: NIST glasses (SRM 612 and 614) and glasses from P&H Developments Ltd., denoted by Trace Glasses SRM-ICP1 for 41 trace elements in a Si-Al-Ca-Na matrix: DLH5 (5 ppm trace elemental concentrations), DLH6 (blank), DLH20 (20 ppm), DLH7 (75 ppm) and DLH8 (150 ppm). In addition, the concentrations of the matrix elements in these glasses were determined by our EMP. For all elements, a natural isotope distribution is assumed. Calibration and data evaluation of the unknown sample were based on a common inherent internal standard, 29Si. For calibration with the various glasses, a sensitivity factor for each of the investigated isotope relative to 29Si was derived from the ratio of the two corresponding ion intensities modified for the known elemental concentrations and isotopic abundances. This ratio has been obtained as the average of a series of individual ratios, usually more than 10, which were calculated from the ion intensity versus time profile within a single laser ablation procedure. The relative elemental concentration was again derived considering the natural isotopic abundances. For the conversion of the relative to absolute elemental concentrations, the absolute elemental concentration of the internal standard Si was measured by the EMP. For this purpose, the corresponding thin-section was repolished. Afterwards, EMP multi-spot analyses were performed in the nearest vicinity of the ablation crater yielded the required Si concentration. In this way, differences in the overall ion production and detection pathway, including different absorption properties of the sample and the reference glasses, were corrected. For the element concentration, a maximum error ranging from 10% for the heaviest isotope (205Tl) to 30% pronounced only for the lightest isotope (6Li) was considered. Also, for the reduction of the error, the results based on 6Li and 7Li as well as 10B and 11B were averaged. To select appropriate spots in a relatively homogeneous garnet (at the surface) for the laser ablation, element concentration maps were prepared before the LA-ICP-MS analyses.

MINERALOGY OF THE SKARN

As mentioned above, the Kal-e Kafi skarn is restricted to thin marble interlayers of schist and these layers were completely replaced by skarn minerals. Garnet is the dominant anhydrous calcsilicate, being ubiquitously present within the skarn. In hand specimen this mineral is pale brown to yellow and in some samples is dark brown in color. Clinopyroxene is not as dominant as garnet and it is always replaced by garnet, epidote, tremolite, actinolite, chlorite, quartz, and calcite. These second minerals occur in subordinate amounts, so various anhydrous and hydrous minerals occur during the sequential stages of the skarn formation.

PETROGRAPHY

More than 90% of the studied sample is consisted of garnet. Then, the most abundant minerals in this sample are clinopyroxene, calcite, chlorite, and quartz. Under the microscope, most of garnets are small (0.5–2 mm in diameter), euhedral, colorless to pale yellow crystals. Some crystals have euhedral shape with internal polysynthetic twining parallel to crystal growth surfaces (Fig. 2a). Birefringent cores with isotropic rims also occur (Fig. 2b). Rhythmically banded textures are characteristics of garnet formation in prograde stage of hydrothermal alteration (Gaspar et al., 2008). Thus, it could be elucidated that garnets in the sample are prograde. In some cases, the euhedral faces of intergrown garnets are pointing to relatively coarse grained quartz and calcite aggregates (Fig. 2a). It is suggested that such aggregates represent former fluid channels. The major elemental chemistry of the main silicate minerals of the studied skarn samples (garnet and clinopyroxene) is shown in Fig. 3. Clinopyroxene always shows poikiloblastic texture in calcite and garnet. In some cases, they are grown as amorphous small crystals in calcite and it seems that they are the reaction product of Si bearing fluids with carbonate ground mass (Fig. 2c). Also, the remnants of small clinopyroxene aggregating in large isotropic garnet crystals show that the clinopyroxenes are converting to garnet (Fig. 2d). They are typically Fe-rich and dominated by the hedenbergite end-member (Table 2). All the studied garnets are dominated by the grossular-andradite solid solution with only minor amounts of Mn, Fe^{2+}, Cr and Mg present, and show major element zonation, indicated by the variations in grey scale (mean atomic number contrast) of BSE images (Fig. 4b). One of the most typically zoned garnets was chosen to determine the oscillatory zonation pattern of grandite garnet in this skarn system and three garnets have been chosen to demonstrate REE behavior in these minerals during the skarn evolution.

RESULTS

Major-Element Zonation

Compositional zoning of minerals, especially garnet is frequently observed in skarns (Meagher, 1982) and might be resulted from hydrothermal overgrowths on contact metamorphic minerals and variations in P, T and XCO_2 concentrations of Fe^{3+} and Al^{3+}, or kinetic factors (Lee and Atkinson, 1985; Jamtveit and Hervig, 1994). The petrographic studies displayed oscillatory zoning of garnet (Fig. 3a). Figure 3b presents the back-scattered electron image (BSE) of an euhedral garnet having a fairly homogeneous and xenomorphic

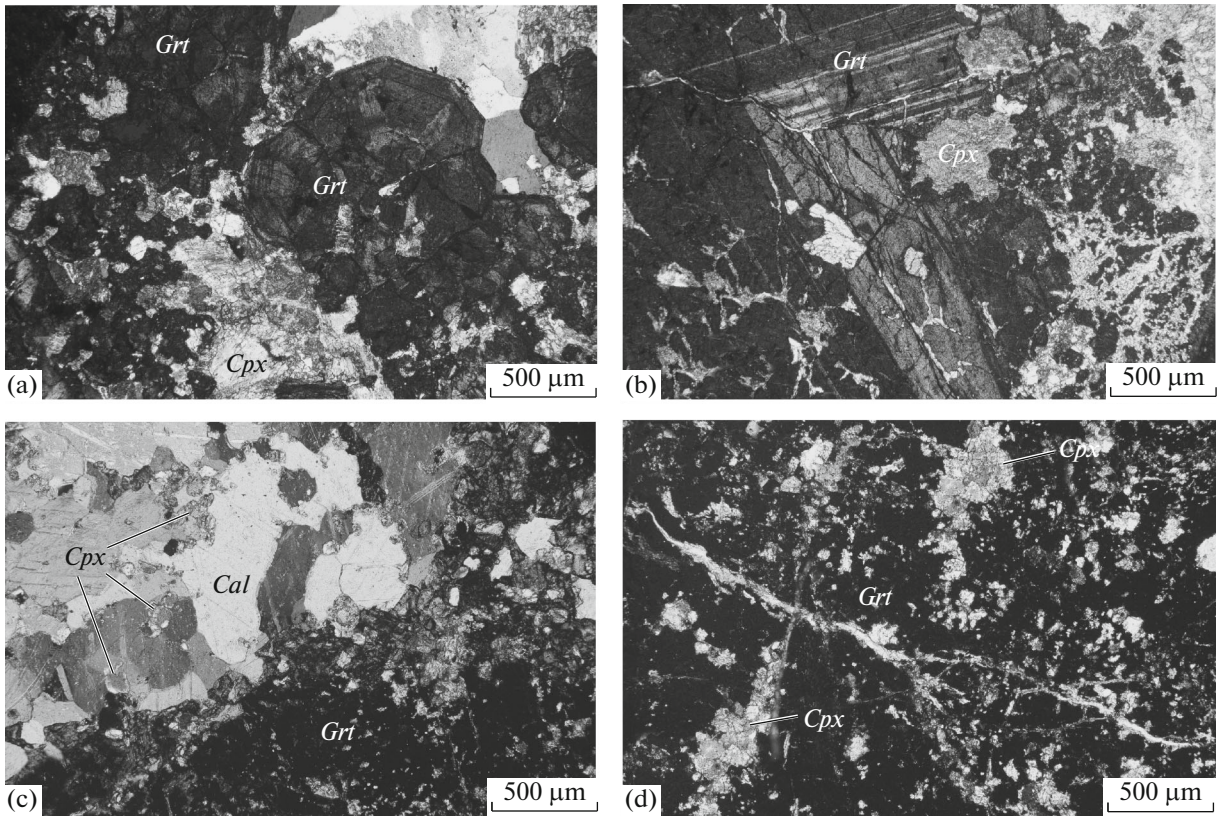

Fig. 2. (a) Growth of euhedral garnet faces with sector twining toward the interior of the cavity. Spaces around the euhedral faces of the garnet crystal are now totally filled with quartz and calcite. (b) Growth of the optically isotropic garnet over the birefringent core. There is some clinopyroxene inclusion in this garnet core. (c) Small poiciliblast of clinopyroxenes are grown in the carbonate minerals. (d) Remnants of clinopyroxene aggregate are observed in the isotropic garnet. Abbreviations are after (Whitney and Evans, 2010).

core surrounded by a striking oscillatory zonation with sharp boundaries between layers of different composition. In this image, brighter areas had more andradite content. A profile obtained from 20 spot analysis (Figs. 3c and 4) reveals major element zoning correlated with the zoning observed in the optical microscopic and BSE images (Figs. 3a and 3b). The data are presented in Table 1. The compositional variation of the garnet can be roughly described as a binary mixture of grossular ($Ca_3Al_2Si_3O_{12}$) and andradite ($Ca_3Fe_2Si_3O_{12}$) with a minor contribution of spessartine ($Mn_3A_{l2}Si_3O_{12}$). They range in composition vary from Al_2O_3 = 0.13 to 5.71 wt %, Fe_2O_3 = 5.45 to 19.25 wt %, and MnO = 0.27 to 0.56 wt % respectively. The major chemical variations point out an inverse relation between Al_2O_3 and Fe_2O_3. Also, the similarity between the Al_2O_3, SiO_2, CaO and Fe_2O_3 with the FeO pattern is clear. (Figs. 3c and 4, Table 1). The garnet crystal shows symmetrical but complex profile with variation in Al_2O_3 and Fe_2O_3 from core to rim. Four oscillatory zonings, it can be observed that which item corresponds to sharp color zoning in the BSE images (Fig. 3c). As it could be seen in Fig. 3c and Table 1, the oscillatory zoning ranges from 68.26 to 99.17 of andradite mole % and a corresponding variation of grossular from 0.00 to 30.43. There is a significant relationship between anisotropy and the $Fe^{3+}/(Fe^{3+}+Al)$ ratio. In general, andradite garnets (Adr > 90) are isotropic, whereas intermediate grandites are anisotropic (Gaspar et al., 2008). Andradite-rich garnets commonly show epitaxial growth on the preexisting garnets with higher grossular content (Figs. 2b and 3). The feature of all these zonation profiles is an abrupt change in chemistry from one intracrystal layer to another. The sharp contacts have been considered as an indication of rapid crystal growth or rapid changes in the composition of the hydrothermal solution. There is a wide range of birefringence colors (from very dark to pale grey) in the garnets. The electron microprobe analysis shows a strong correlation between the birefringence and the composition (Figs. 3b,c). The isotropic zones have a composition close to pure andradite (X_{and}^{EMP} = 0.83–0.99), whereas the anisotropic zones reflect an intermediate composition (X_{and}^{EMP} = 0.68–0.78) (Table 1). This is consistent with a majority of skarn systems, in which, early prograde garnets tend to be Al-rich and later or retro-

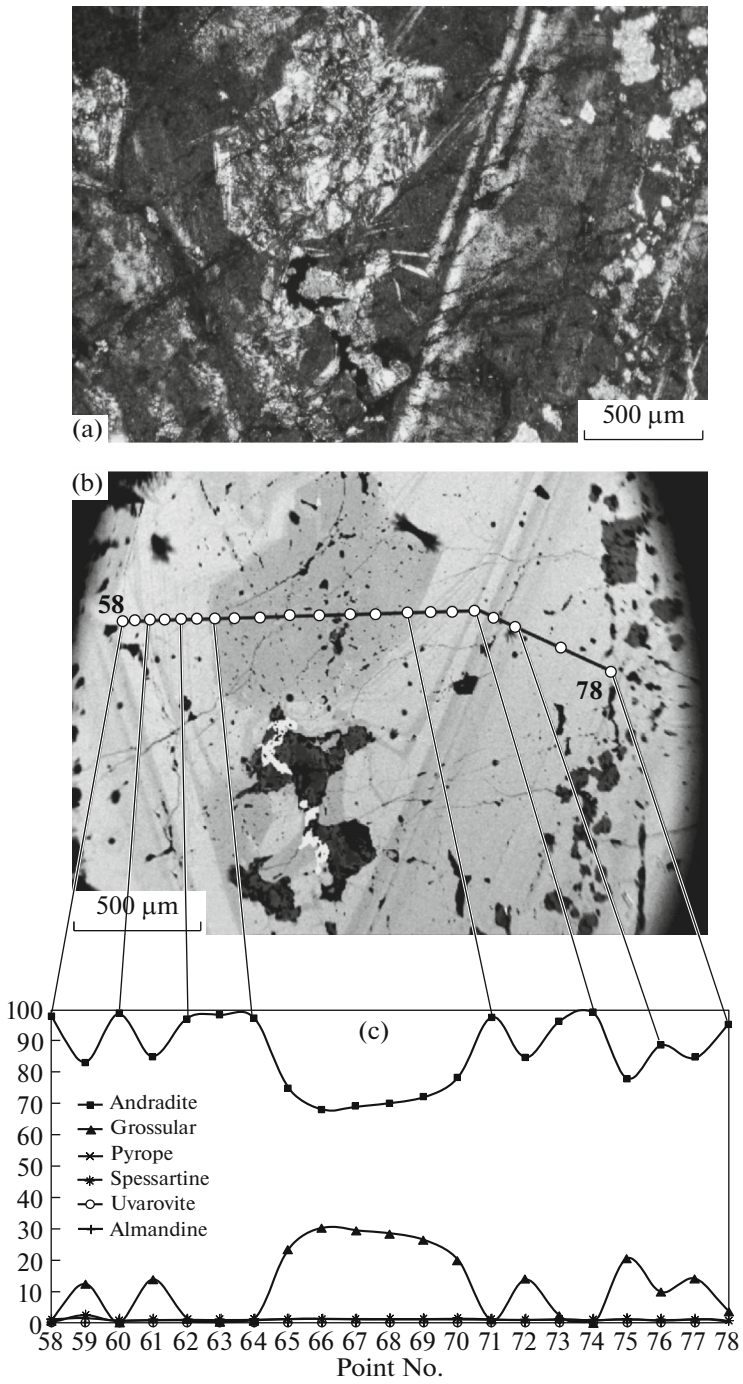

Fig. 3. (a) The studied garnet under XPL which shows distinct oscillatory zonation. In general, the core and brighter areas, have more grossularitic composition. (b) The back-scattered electron image (BSE) of the euhedral garnet that has a fairly homogenous core surrounded by a striking oscillatory zonation with sharp boundaries between layers of different composition. The black line indicates the line profile analysis from rim (point 59) to rim (point 78). (c) The zonation profile (along line 3b) for main garnet end members. Four oscillatory parts are divided and shown by black lines.

grade ones tend to be Fe-rich (Einaudi et al., 1981; Nakano et al., 1989; Meinert, 1992, 1997).

According to Fig. 5a, the Ca content is approximately homogeneous in all parts of this crystal. On the basis of Fig. 5b, this garnet has no Mg content and this element is only increased in parts with clinopyroxene inclusions. Image 5c reveals zonation alternating between grossular-rich core (grey) and andradite rich rim (light grey), with andradite zones forming majority of the garnet. The Mn pattern is in contrast with

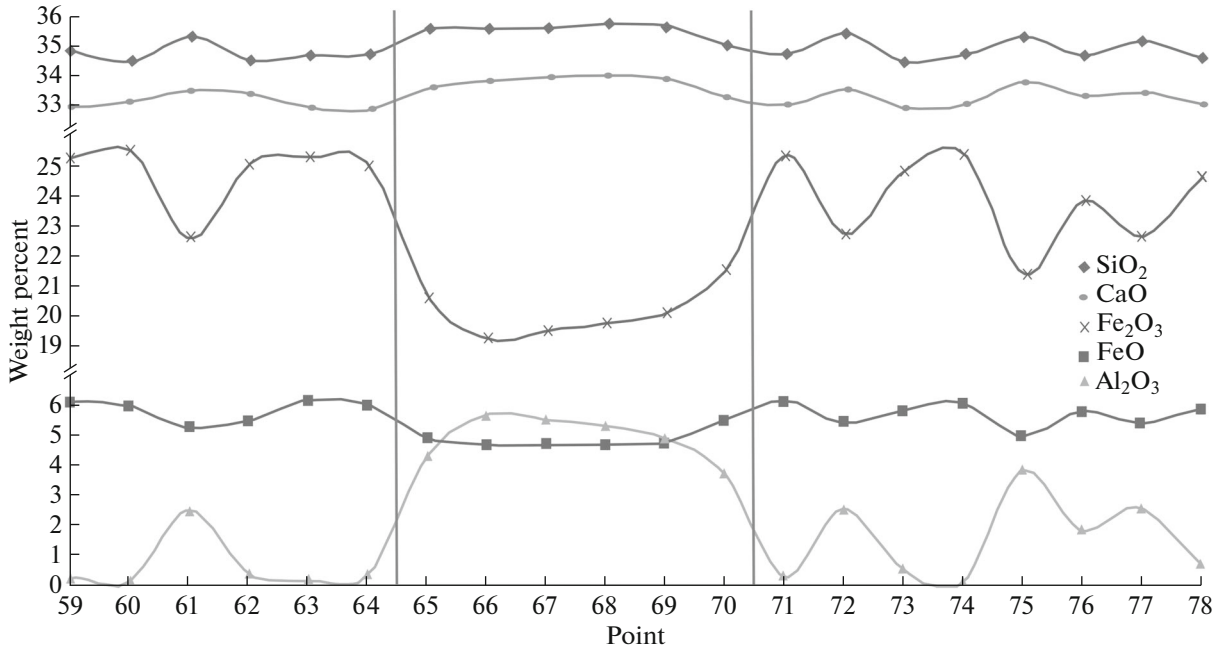

Fig. 4. The poor positive correlation between SiO_2 and CaO with Al_2O_3 and also Fe_2O_3 with FeO. SiO_2 and CaO increase slightly with increase of Al_2O_3 in the core. On the other hand, these oxides have negative correlation with Fe_2O_3 and FeO. The two parallel blue lines show the boundary of the garnet core.

Fe, so where Fe is increased, Mn will be depleted and vice versa (Figs. 5c and 5d).

REE PATTERN OF GARNET

To determine REE behavior of the studied garnets, three garnets were picked out and three representative points of each mineral were subjected to analysis by LA-ICP-MS. Each garnet has a homogenous core overgrown by the oscillatory zoned garnet interrupted by zones with resorbed inner margins and more significant changes in chemistry. For each garnet, two points of grossular-rich (at the core) and one point of more andraditic (in the rim) part were analyzed. The rare earth element ICP-MS analyses of each sample were normalized to the chondrite values of Masuda et al. (1973) and Masuda (1975). Y was included as a pseudolanthanide and it was plotted between Dy and Ho.

These garnets have nearly similar REE behavior, that is, they are LREE-rich (especially in Pr,Nd and Sm) having flat to depleted MREE and HREE patterns.

REE Fractionation in the Garnet

Trace element (especially REEs) incorporation into the mineral structure has been reviewed by several scholars (e.g. Jamtveit et al., 1993; Jamtveit and Hervig, 1994; Smith et al., 2004; Gasper et al., 2008). Ling and Liu (2003) concluded that redistribution of REE in skarn forming processes is mainly controlled by three factors: (a) REE concentrations in original rocks; (b) REE concentrations in the fluid, and (c) the ability of the REE which is released during alteration. Each of these factors could have a relative impact on the fate of the REE during different stages of skarnification.

Also as Smith et al. (2004), these mechanisms are interpreted in the literature for process of partitioning of trace element into the mineral:

1. Removal of elements from the fluid (including the breakdown of aqueous complexes);

2. Sorption onto a growth surface;

3. Incorporation of elements into the bulk mineral via a substitution mechanism and diffusion through the surface layer;

4. Solution of substituted cations into the aqueous fluid.

Thus, trace elements incorporation into mineral structure will be a function of chemical composition, pressure, and temperature of the system in addition to surface complexion, crystal chemistry, and the relative rates of mineral growth and diffusive re-equilibration in the bulk crystal.

Shannon (1976) indicated that ionic valence, ionic radius, and temperature are important factors controlling alteration during rock-fluid interaction. The higher the ionic valence and temperature are, the more stable the REE complexes will be, while the larger the ionic radius, the less stable are the REE complexes (Bao and Zhao, 2003). Ling and Liu (2003) showed that REE characteristics of skarns are con-

Table 1. Representative electron microprobe (EMP) analysis for studied garnet

Point Description	59 Iso.	60 Iso.	61 Iso.	62 Iso.	63 Iso.	64 Iso.	65 Aniso.	66 Aniso.	67 Aniso.	68 Aniso.	69 Aniso.
SiO_2	34.77	34.48	35.30	34.49	34.66	34.70	35.54	35.55	35.61	35.71	35.63
TiO_2	0.01	0.00	0.01	0.00	0.00	0.00	0.00	0.01	0.16	0.00	0.00
Al_2O_3	0.31	0.18	2.53	0.45	0.24	0.40	4.32	5.71	5.56	5.34	4.93
Fe_2O_3	25.22	25.45	22.59	25.06	25.26	24.96	20.60	19.25	19.51	19.77	20.14
FeO	6.19	5.98	5.29	5.53	6.20	6.03	4.95	4.72	4.74	4.74	4.81
MnO	0.35	0.29	0.32	0.31	0.32	0.38	0.44	0.46	0.48	0.45	0.46
MgO	0.01	0.00	0.00	0.00	0.01	0.00	0.00	0.00	0.00	0.00	0.00
CaO	32.95	33.19	33.51	33.41	32.92	32.89	33.59	33.80	33.95	34.00	33.87
Na_2O	0.01	0.00	0.02	0.00	0.00	0.00	0.00	0.02	0.04	0.03	0.00
K_2O	0.00	0.00	0.00	0.00	0.00	0.00	0.00	0.00	0.01	0.00	0.00
Cr_2O_3	0.00	0.01	0.00	0.00	0.01	0.00	0.013	0.00	0.00	0.00	0.00
Total	99.85	99.61	99.59	99.28	99.65	99.38	99.48	99.56	100.07	100.07	99.87
Si	2.99	2.98	3.00	2.98	2.99	2.99	2.99	2.97	2.96	2.97	2.98
Al^{IV}	0.00	0.02	0.00	0.01	0.00	0.00	0.00	0.02	0.03	0.02	0.01
T-Total	3	3	3	3	3	3	3	3	3	3	3
Al^{VI}	0.02	0.00	0.27	0.03	0.01	0.04	0.44	0.56	0.54	0.53	0.49
Ti	0.00	0.00	0.00	0.00	0.00	0.00	0.00	0.00	0.01	0.00	0.00
Cr	0.00	0.00	0.00	0.00	0.00	0.00	0.00	0.00	0.00	0.00	0.00
$Fe^{3+(VI)}$	1.63	1.65	1.44	1.63	1.64	1.62	1.30	1.21	1.22	1.24	1.26
$[R^{3+}]^{VI}$	2	2	2	2	2	2	2	2	2	2	2
Fe^{2+}	0.44	0.43	0.37	0.40	0.44	0.43	0.34	0.33	0.33	0.33	0.33
Mn	0.02	0.02	0.02	0.02	0.02	0.02	0.03	0.03	0.03	0.03	0.03
Mg	0.00	0.00	0.00	0.00	0.00	0.00	0.00	0.00	0.00	0.00	0.00
Ca	3.04	3.07	3.05	3.09	3.04	3.04	3.03	3.02	3.03	3.03	3.03
$[R^{2+}]^{VIII}$	3	3	3	3	3	3	3	3	3	3	3
Almandine	0.00	0.00	0.00	0.00	0.00	0.00	0.00	0.00	0.00	0.00	0.00
Andradite	98.09	98.79	85.07	97.21	98.44	97.50	75.22	68.26	69.14	70.25	72.27
Grossular	0.78	0.27	14.00	1.84	0.51	1.38	23.51	30.43	29.56	28.54	26.47
Pyrope	0.09	0.02	0.00	0.00	0.06	0.00	0.00	0.03	0.00	0.01	0.00
Spessartine	1.02	0.86	0.92	0.92	0.94	1.11	1.23	1.25	1.29	1.21	1.24
Uvarovite	0.01	0.06	0.01	0.03	0.04	0.00	0.05	0.03	0.00	0.00	0.02

Table 1. (Contd.)

Point Description	70 Aniso.	71 Iso.	72 Slightly Aniso.	73 Slightly Aniso.	74 Slightly Aniso.	75 Aniso.	76 Aniso.	77 Slightly Aniso.	78 Slightly Aniso.
SiO_2	35.01	34.72	35.39	34.44	34.70	35.27	34.68	35.13	34.56
TiO_2	0.10	0.00	0.01	0.00	0.00	0.08	0.00	0.01	0.02
Al_2O_3	3.78	0.36	2.58	0.57	0.13	3.82	1.91	2.61	0.75
Fe_2O_3	21.55	25.30	22.69	24.84	25.36	21.38	23.77	22.66	24.64
FeO	5.55	6.19	5.47	5.87	6.12	5.01	5.84	5.46	5.94
MnO	0.49	0.38	0.34	0.37	0.27	0.41	0.36	0.37	0.27
MgO	0.01	0.01	0.01	0.02	0.01	0.00	0.02	0.00	0.00
CaO	33.29	33.05	33.53	32.96	33.02	33.75	33.37	33.42	33.01
Na_2O	0.00	0.00	0.00	0.00	0.00	0.00	0.00	0.03	0.00
K_2O	0.00	0.00	0.00	0.01	0.00	0.01	0.00	0.00	0.00
Cr_2O_3	0.00	0.09	0.01	0.02	0.00	0.00	0.01	0.00	0.00
Total	99.81	100.04	100.05	99.13	99.62	99.76	99.96	99.72	99.23
Si	2.90	2.98	2.99	2.98	2.99	2.97	2.96	2.98	2.98
Al^{IV}	0.09	0.01	0.00	0.01	0.00	0.02	0.03	0.01	0.01
T-Total	3	3	3	3	3	3	3	3	3
Al^{VI}	0.30	0.02	0.26	0.04	0.01	0.37	0.16	0.26	0.06
Ti	0.00	0.00	0.00	0.00	0.00	0.00	0.00	0.00	0.00
Cr	0.00	0.00	0.00	0.00	0.00	0.00	0.00	0.00	0.00
$Fe^{3+(VI)}$	1.42	1.63	1.44	1.61	1.64	1.35	1.52	1.44	1.60
$[R^{3+}]^{VI}$	2	2	2	2	2	2	2	2	2
Fe^{2+}	0.48	0.44	0.38	0.42	0.44	0.35	0.41	0.38	0.42
Mn	0.03	0.02	0.02	0.02	0.02	0.03	0.02	0.02	0.02
Mg	0.00	0.00	0.00	0.00	0.00	0.00	0.00	0.00	0.00
Ca	2.96	3.04	3.04	3.05	3.05	3.05	3.05	3.04	3.05
$[R^{2+}]^{VIII}$	3	3	3	3	3	3	3	3	3
Almandine	0.00	0.00	0.00	0.00	0.00	0.00	0.00	0.00	0.00
Andradite	78.40	97.78	84.83	96.41	99.17	78.13	88.77	84.70	95.43
Grossular	20.16	1.02	14.09	2.31	0.00	20.70	10.04	14.21	3.74
Pyrope	0.07	0.05	0.07	0.11	0.05	0.02	0.11	0.02	0.04
Spessartine	1.36	1.11	0.96	1.09	0.77	1.14	1.03	1.06	0.80
Uvarovite	0.02	0.04	0.05	0.08	0.01	0.00	0.04	0.00	0.00

trolled by garnets. One of the most important reasons for substitution of REE in skarn garnets is similarity between ionic radius of Ca^{2+} and trivalent REE in eight-fold co-ordination (Shannon, 1976) especially for Ca, Pr and Nd. The results of LA-ICP-MS analysis of the studied garnets are presented in Table 3.

The REE pattern of these garnets shows negative anomaly for La, Ce and Eu to some extent. It also indicates positive anomaly for Pr, Nd and Sm and negative one to flat pattern for Gd to Lu (Fig. 6). In general, as it was mentioned by Gaspar et al. (2008), Al-rich garnets have more ∑REE whereas Fe-rich garnets (Adr > 90) have much lower ∑REE.

The inferred comparatively weak partitioning of La into garnet may arise from a greater mismatch in ionic radius between La and Ca than between Ce, Pr, Nd

Table 2. Representative analysis of Clinopyroxene

Point	143	144	145	146	147	148
SiO_2	51.15	50.94	50.47	50.39	50.88	50.94
TiO_2	0	0	0	0	0	0
Al_2O_3	0	0	0.10	0.10	0.02	0
FeO	17.45	18.37	19.36	19.81	17.56	17.63
MnO	0.84	1.61	0.57	0.46	0.53	1.41
MgO	7.62	7.12	6.4	6.37	7.53	7.19
CaO	23.37	23.02	22.59	22.48	23.00	22.73
Na_2O	0.40	0.47	0.64	0.63	0.61	0.63
K_2O	0.01	0	0	0.00	0.01	0
Total	100.9	101.55	100.16	100.28	100.18	100.56
WO	48.36	47.42	48.00	47.64	48.30	47.73
EN	22.06	20.41	18.91	18.80	22.02	21.02
FS	29.56	32.16	33.08	33.54	29.67	31.24

Wo: Wollastonite; EN: Enstatite; FS: Ferrosilite.

and Ca (16). Coupled with this, complexes of La^{3+} with Cl^- and F^- are predicted to be more strongly associated than those of Nd^{3+} and Sm^{3+} by the models of Haas et al. (1995). Kato (1999)believes that depletion of La is probably due to the lanthanide tetrad effect (Masuda and Ikeuchi, 1979).

Under oxidized and neutral to moderately acidic conditions, unlike other trivalent REE ions, Ce^{3+} could be readily oxidized to Ce^{4+} and then precipitated in the form of CeO_2 or absorbed onto the surface, and/or into the structure of secondary minerals (Goldberg et al., 1963; Piper, 1974; Elderfield et al., 1981; Liu et al., 1988). The differentiation of Ce with the other REE suggests that Ce has been less mobile during hydrothermal alteration. Also, the negative Ce anomaly reflects a striking Ce depletion of ancient seawater under which the protolith of limestone was deposited (Kato, 1999).

As Eu exists in aqueous fluids in either divalent or trivalent states, redox condition of granitic system may influence the Eu redox equilibrium and as a result makes Eu anomaly (Kato, 1999). Besides, the negative Eu anomalies might be explained by the absence of ligands such as Cl^-, capable of transporting Eu^{2+} (Gaspar et al., 2008).

The increasing stability of aqueous REE complexes with atomic number (wood, 1990; Hass et al., 1995) accounts for slight decrease in normalized REE abundance from Ho to Lu; however, as pointed out by Bau (1991), whole rock REE patterns should not vary significantly during hydrothermal or metamorphic alteration. Only long fluid residence or high water/rock ratios (i.e. fluid dominant system (W/R >102) can significantly change the REE content of the rocks, such as in the case of intense infiltration metasomatism (Bau, 1991; Lottemoser, 1992). Heterogeneous distribution of REE on surface of growing garnet crystals may have been an important factor in the origination of these garnets' REE patterns (Whiteny and Olmsted, 1998).

Table 3. LA-ICP-MS analysis of garnets from Kal-e Kafi skarn

Sample No. Mineral	kaB-1a *Grt*	kaB-1b *Grt*	kaB-1c *Grt*	kaB-2a *Grt*	kaB-2b *Grt*	kaB-2c *Grt*	kaB-3a *Grt*	kaB-3b *Grt*	kaB-3c *Grt*
La	2.18	8.85	3.2	6.73	28.29	1.38	6.46	9.35	10.22
Ce	15.72	16.6	22.89	35.64	76.8	6.82	30.08	49.81	17.39
Pr	5.05	3.17	5.16	7.84	14.18	2.22	5.65	10.63	3.13
Nd	44.08	24.1	31.27	47.34	88.68	21.54	28.32	63.75	23.55
Sm	18.76	7.24	10.33	10.39	27.13	7.94	6.44	17.49	10.51
Eu	3.27	2.13	2.08	2.79	6.2	2.24	2.34	3.18	3.16
Gd	21.08	6.57	11.43	8.22	24.8	7.42	6.95	19.24	10.85
Tb	3.32	0.89	1.73	0.99	2.98	1.06	0.97	2.93	1.62
Dy	22.05	4.99	11.36	5.8	15.76	6.22	6.21	19.03	10.8
Ho	4.31	0.9	2.35	1.01	2.5	1.2	1.21	3.39	2.09
Er	11.09	2.2	6.22	2.5	5.67	2.93	3.19	9.66	5.08
Tm	1.44	0.27	0.81	0.29	0.63	0.37	0.38	1.23	0.64
Yb	7.9	1.67	5.05	1.6	3.42	2.22	2.27	6.93	3.51
Lu	1.12	0.23	0.74	0.2	0.43	0.32	0.31	1.02	0.48
∑REE	171.34	78.45	114.57	131.31	297.46	63.81	100.75	217.58	103.01

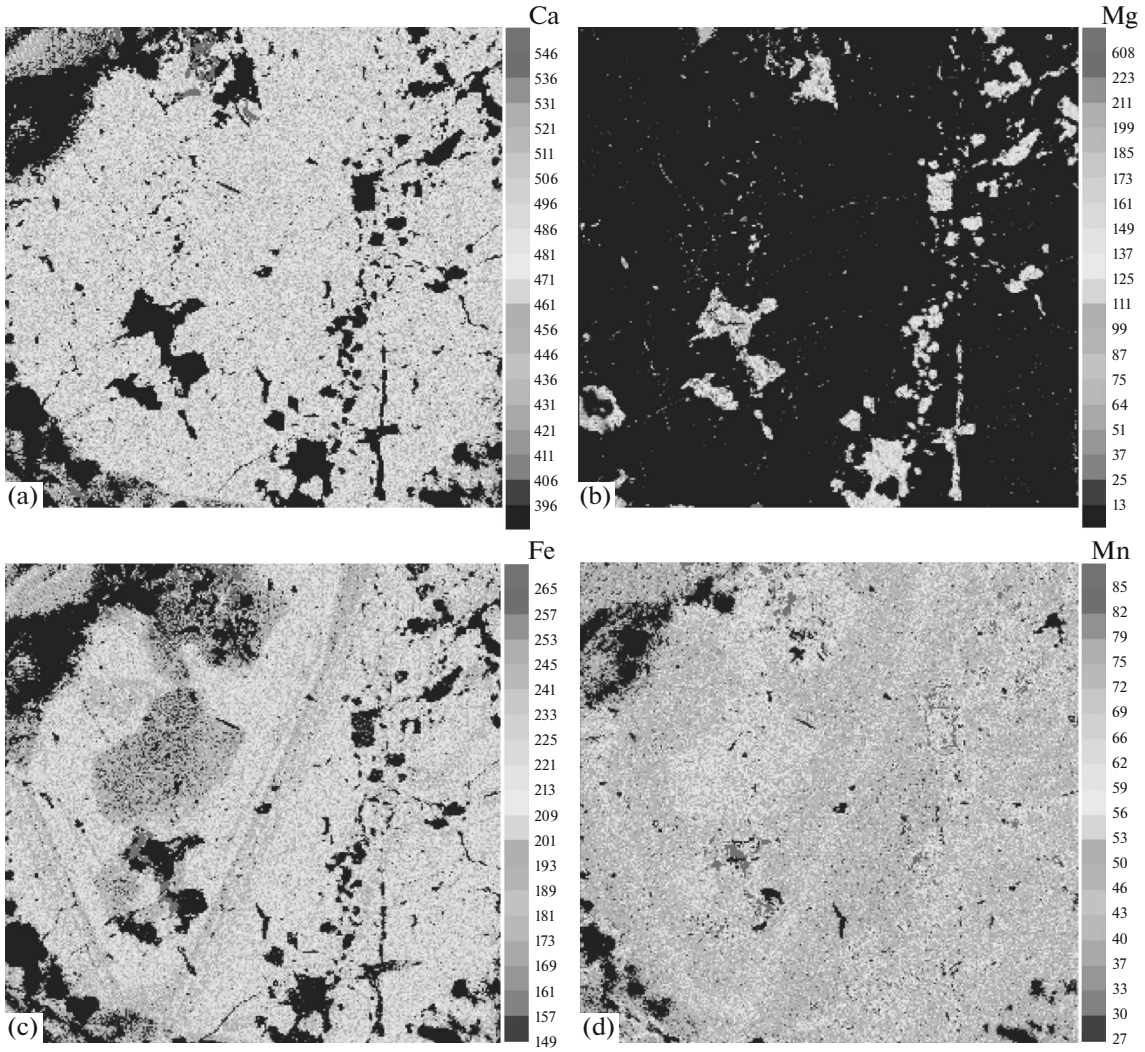

Fig. 5. Ca, Mg, total Fe and Mn concentrations X-ray map in garnet obtained on a CAMECA SX100 EMP.

DISCUSSION

In metamorphic rocks, chemical zoning in garnet is one of the most important tools for constraining P-T histories during orogenesis (e.g. Spear, 1993). This is based on the assumption that the chemical profile preserved in garnet reflects equilibrium compositions in different times during garnet growth. While oscillatory zoning in metamorphic minerals is not common. It is frequently recorded from fluid-dominated environments and mineralized hydrothermal systems such as skarn deposits (e.g. Smith et al., 2004). In these systems, the garnet zoning patterns reflect the alteration history during fluid–rock interaction, and thus, provide crucial information about the processes of a developing hydrothermal system (e.g. Jamtveit et al., 1993). Oscillatory zoning in garnet has been widely reported (Lessing and Standish, 1973; Murad, 1976; Jamtveit et al., 1995; Akizuki et al., 1984, Intayot et al., 2007, Dziggel et al., 2009, Caddick et al., 2010, Jansson and Allen, 2013). Several models have been proposed to explain such zoning. Attempts to explain complex mineral zoning pattern commonly have been based on two different assumptions: (1) the zonation is a result of internal crystal growth process such as by self-organization (Haase et al., 1980,Heurex and Fowler, 1994) or (2) the zonation mainly reflects changes in the external geological environment during crystal growth such as a variable mass flux through an open system or fluctuation in variables such as temperature and pressure (Jamveit et al., 1995; Haase et al., 1980; Yardley et al., 1991).

The origin of complex multiscale zonality patterns in grandite garnets is still questionable. Ivanova et al. (1998) presented three main causes for this phenomenon. These hypotheses are:

1. Any compositional zonality is the result of abrupt or continuous changes in the composition of a hydro-

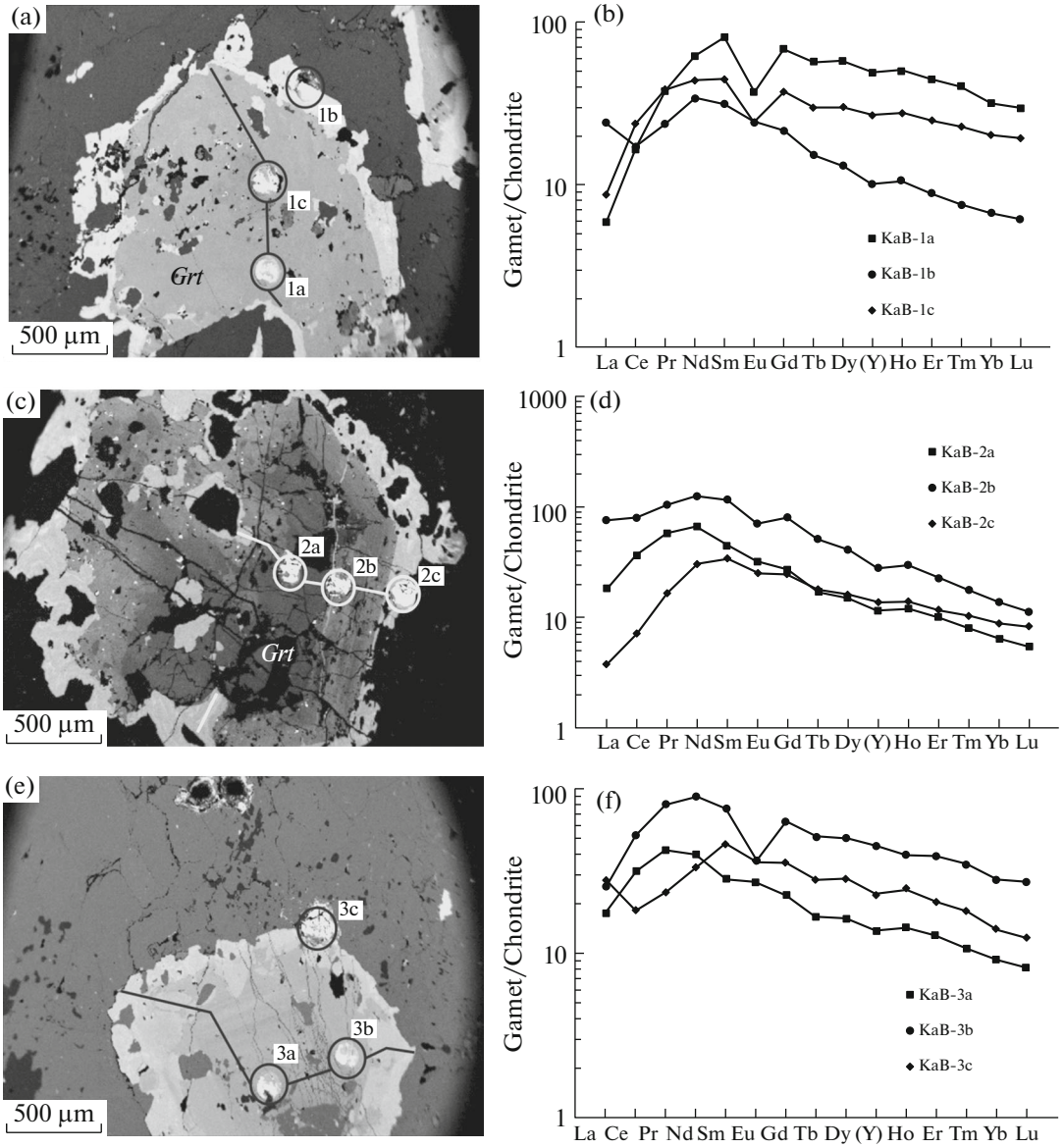

Fig. 6. The BSE images of three garnets of the KaB sample and their REE behavior. On the basis of microprobe analysis, darker areas in BSE images of all garnets, have more grossularitic and the brighter areas (at the rim) have more andraditic composition. The REE pattern of these garnets shows negative anomaly for La, Ce and Eu to some extent, it also shows positive anomaly for Pr, Nd and Sm and negative to flat pattern for Gd to Lu.

thermal solution as well as in p-T conditions occurring during crystal growth. (e.g. García-Casco et al., 2002).

2. Fine growth zonality originates from the non-stationary growth dynamics (e.g. Jamtveit and Anderson, 1992).

3. Post-growth exsolution is the reason of formation of the wave-like or tweed-like texture.

Ivanova et al. (1998) accepted the first and the second hypotheses and rejected the third and presented some reasons for rolling out that hypothesis in their paper.

Also, Spear (1993) proposed two major aspects of chemical zoning in garnet. First, compositional differences in the layer arise because of changing external conditions such as changing P-T conditions, or a change in the local bulk composition of the rock. Second, diffusion is a modification of a pre-existing garnet zoning by the process of volume diffusion. As with growth zoning, the driving force for the diffusion of zoning is typically a change in external conditions, in contrast, diffusion zoning requires no growth or consumption of the crystal. Moreover with growth zoning, there is no post-growth modification of the garnet

composition whereas with diffusion zoning, modification may occur during and following growth.

The central idea behind growth zonation of garnet is the point that the composition of material supplied to the garnet rim change with time as the garnet grows. This new material is incorporated into the garnet and a shell of a new composition is produced. As soon as diffusion is sufficiently slow, the composition of these shells will not change and the zoning profile will faithfully record the composition of the rim of the garnet at the time it was growing.

An interpretation of isochemical or near-isochemical growth controlled by diffusion in the local environment during the initial stages of contact metamorphism, followed by metasomatic growth as a result of the infiltration of an external fluid is entirely consistent with the textural evidence from the garnets. The ingress of fresh batches of granite-derived aqueous fluid led to major chemical overstepping of the andradite-forming equilibria, super-saturation, and the formation of oscillatory zoned rims as a result of enrichment-depletion cycles in garnet components in solution during growth (Ortoleva et al., 1987; Jamtveit and Andersen, 1992; Jamtveit et al., 1993; Holten et al., 1997, 2000). One of the most important microscopic signatures of these garnets is the regular oscillatory zoning that is interrupted by broad zones that display dissolution of earlier zones on their inner margins, suggesting significant externally controlled changes in the chemical conditions at these stages. In these garnets, the outer zone that surrounds the mineral is Fe-enriched. Scholars such as Jamtveit and Hervig (1994) suggest that boiling is the main reason for oscillatory zoning, but in the absence of boiling evidences, such variations might occur as a result of alternation between internally and externally buffered fluid compositions during pulsed fluid flow (Yardley et al., 1991). The change in the relative iron content of the zones, with evidence of dissolution on their inner margins, probably arises from the change in iron content between the more saline fluids and less saline fluids. The Fe content of skarn-forming fluids is closely related to their total salinity (Kwak et al., 1986).

The grandite garnets from the Kal-e Kafi area have distinguishing characteristics of the crystal growth process. Oscillatory zoning in the grandite garnet is commonly resulted from variation in Al^{3+} and Fe^{3+} contents (Figs. 3 and 5), but the distribution of trace elements (for instance Ti, As and Mn) can also be inhomogeneous (Jamveit et al., 1995). The oscillatory fluctuations in grossular-andradite component suggest that variation in the Al and Fe^{3+} contents of a hydrothermal fluid have controlled the zoning and the Mn and Ti contents of these garnets are low.

Detailed chemical analyses of the oscillatory zoning in the grandite garnet from the Kal-e Kafi area showed fluctuation in chemical composition. The grandite garnets normally displayed core with intermediate composition and oscillatory Fe-rich zones at the rim. A change in fluid composition during the garnet growth may cause the garnet stop growing temporarily or keep growing but in a much slower rate allowing the Al to precipitate rather than Fe. Detailed study of the oscillatory zoning in the grandite garnet of Kal-e Kafi area recommends that the garnet developed during early metasomatism including monzonite to monzodiorite granitoid body intrusion into the Anarak schist- marble interlayers. During this metasomatic event, Al, Fe and Si in the fluid reacted with Ca in the carbonate rocks to form the grandite garnet. The oscillatory zoning in the garnet probably reflects an oscillatory change in the fluid composition which may be internally and/or externally controlled.

Mechanism of Garnet Growth

Intrusion and cooling of H_2O rich magmas at shallow crustal levels invariably lead to the liberation of large amounts of fluids into the surrounding country rocks. During contact metamorphism and hydrothermal alteration of carbonate bearing rocks, calcic garnets grow under a variety of physicochemical conditions. Variations in physical conditions also fluid composition and protolith compositions will affect the balance between dissolution of calcite and the growth of hydrothermal minerals. Variations in temperature, Fe^{3+} activity, or XCO_2 with time or position in the hydrothermal system could influence the stability of andradite (Taylor and Liou, 1978; Zhang and Saxena, 1991). Such skarn garnets commonly display complex oscillatory chemical zonation patterns (Lessing and Standish, 1973; Jamtveit, 1991). Oscillatory zonation may be a main feature of systems open to fluid flow, and the zonation patterns may provide a continuous record of the physicochemical evolution of the hydrothermal system in which the zoned mineral grew. As shown by Jamtveit (1991), the composition of solid solution systems such as the grossular- andradite binary system may be very vulnerable to small changes in hydrothermal fluid composition.

Early infiltration was pervasive and coeval with more or less ductile deformation, whereas later infiltration mostly occurred along faults and fractures formed during brittle deformation. The backscattered electron (BSE) images (Fig. 4b) show a sharp transition from a relatively more grossularitic core (gr = 20 to 30 mole %) to an andradite-rich rim (gr < 15 mole %). Furthermore, the rim contains several thin layers of more grossular-rich composition that give rise to the oscillatory zonation pattern evident in the BSE image (Fig. 4b). The composition of the grossular-rich layers was largely determined by the local mineral assemble during the periods of slow fluid influx and low crystal growth rates, whereas the composition of more rapidly grown andradite-rich layers reflects infiltration of externally derived hydrothermal fluids.

SUMMARY AND CONCLUSIONS

It can be concluded that the grossular- andradite (grandite) garnets precipitated from hydrothermal solutions are associated with contact metamorphism in the Kal-e Kafi skarn and they show complex oscillatory chemical zonation. Based on optical properties and major elemental chemistry of grandite garnets of the studied sample, different garnets could be identified. These grandite garnets have a birefringent intermediate core with distinct overgrowth of the Fe rich isotropic rim. More Al rich garnets may have formed during early infiltration at the time of Kal-e Kafi granitoid intrusion into the Anarak schist and marble interlayers while the Fe rich garnets have rapidly formed during infiltration metasomatism. Formation of garnet in this skarn system could be internally and externally controlled. Study on the behavior of REE in this skarn system demonstrates that substantial mobility and redistribution of REE can occur in hydrothermal system in carbonate rocks at shallow to intermediate depth of the continental crust. The resulting REE patterns can be used to infer the geochemical processes involved in skarn formation, thus, REE studies are potentially useful for elucidating the origin of skarns in other areas.

ACKNOWLEDGMENTS

This study was financially supported by Isfahan University, faculty of science, department of geology. The authors wish to thank Professor Hans-Joachim Massonne, Institut für Mineralogie und Kristall chemie, Stuttgart University, for technical assistance. Dr. Thomas Theye from University of Stuttgart and Dr. Mehrdad Pasandi from University of Isfahan are gratefully acknowledged for providing useful comments on the manuscript.

REFERENCES

J. Ahmadian, H. Michael, I. McDonald, M. Regelous, M. R. Ghorbani, and M. Murata, "High magmatic flux during Alpine–Himalayan collision: constraints from the Kal-e-Kafi complex, central Iran," Geol. Soc. Am. Bull. **121**, 857–868 (2009).

M. Akizuki, H. Nakai, and T. Suzuki, "Origin of iridescence in grandite garnets," Am. Mineral. **69**, 896–901 (1984).

D. H. M. Alderton, J.A. Pearce, and P.J. Potts, "Rare earth element mobility during granite alteration: evidence from southwest England," Earth Planet. Sci. Lett. **49**, 149–165 (1980).

Z. Bao and Z. Zhao, "Rare-earth element mobility during ore-forming hydrothermal alteration: a case study of Dongping gold deposit, Hebei Province, China," Chin. J. Geochem **22**, 45–47 (2003).

M. Bau, "Rare earth element mobility during hydrothermal and metamorphic fluid-rock interaction and the significance of the oxidation state of europium," Chem. Geol. **93**, 219–230 (1991).

H. J. Bernhardt, H. J. Massonne, T. Reinecke, J. Reinhardt, and A. Willner, "Digital element distribution maps, an aid in pathological investigations. (Berichte der Deutschen Mineralogischen Gesellschaft), Beihefte zum European," J. Mineral. **7**, 28 (1995).

F. P. Bierlein, "Rare-earth element geochemistry of clastic and chemical metasedimentary rocks associated with hydrothermal sulphide mineralisation in the Olary Block, South Australia," Chem. Geol. **122**, 77–98 (1995).

M. J. Caddick, J. Konopasek, and A. B. Thompson, "Preservation of garnet growth zoning and the duration of prograde metamorphism," J. Petrol. **51**, 2327–2347 (2010).

I. H. Campbell, C. M. Lesher, P. Coad, J. M. Franklin, M. P. Gerton, and P. C. Thurston, "Rare earth element mobility in alteration pipes below massive Cu–Zn-sulfide deposits," Chem. Geol. **45**, 181–202 (1984).

C. C. Clechenko and J. W. Walley, "Oscillatory zoning in garnet from the Willsboro Wollastonite Skarn, Adirondack Mts, New York: a record of shallow hydrothermal processes preserved in a granulite facies terrane," J. Metamorph. Geol. **21**, 771–784 (2003).

G. T. R. Droop, "A general equation for estimating Fe^{3+} concentrations in ferromagnesian silicates and oxides from microprobe analyses using stoichiometries criteria," Mineral. Mag. **51**, 431–435 (1987).

A. K. Dziggel, Wulff, J. Kolb, F. M. Meyer, and Y. Lahaye, "Significance of oscillatory and bell-shaped growth zoning in hydrothermal garnet: evidence from the Navachab gold deposit, Namibia," Chem. Geol. **262**, 262–276 (2009).

M. T. Einaudi, L. D. Meinert, and R. J. Newberry, "Skarn deposits," Econ. Geol., 75th Anniversary Volume, 317–391 (1981).

H. C. J. Elderfield, Hawkesworth, M. J. Greaves, and S. E. Calvert, "Rare earth element geochemistry of oceanic ferromanganese nodules and associated sediments," Geochem. Cosmochim. Acta **45**, 513–528 (1981).

A. J. Fleet, "Aqueous and sedimentary geochemistry of the rare earth elements, in *Rare Earth Element Geochemistry* Ed. by P. Henderson, (Elsevier, Amsterdam, 1984), pp. 343–374.

R. L. García-Casco, A. Torres-Roldán, G. Millán, P. Monié, and J. Schneider, "Oscillatory zoning in eclogitic garnet and amphibole, Northern Serpentinite Melange, Cuba: a record of tectonic instability during subduction," J. Metamorph. Geol. **20**, 581–598 (2002).

M. C. Gaspar, L. D. Knaack, Meinert, and R. Moretti, "REE in skarn system: A LA-ICP-MS study of garnet from the Crown Jewel gold deposit," Geochim. Cosmochim. Acta **72**, 185–205 (2008).

"Geological Map of Kabudan: Geological Survey of Iran, 1 :100000 Series, Sheet 68. 1 : 250000," (Technoexport, 1984), No. H7.

R. Giere, "Zirconolite, allanite and hoegbomite in a marble skarn from the Bergell contact aureole: implications for mobility of Ti, Zr and REE," Contrib. Mineral. Petrol. **93**, 459–470 (1986).

E. D. Goldberg, M. Koide, R.A. Schmitt, and R.H. Smith, "Rare-earth distributions in the marine environment," J. Geophys. **68**, 4209–4217 (1963).

M. A. Gouveia, M. I. Prudencio, M. O. Figtueiredo, L. C. J. Pereira, J. C. Waermborgh, I. Morgado, T. Pena, and A. Lopes, "Behavior of REE and other trace and major elements during weathering of granitic rocks, Evora, Portugal," Chem. Geol. **107**, 293–296 (1993).

C. S. Haase, J. Chadam, D. Feinn, and P. Ortoleva, "Oscillatory zoning in plagioclase feldspar," Science **209**, 272–274 (1980).

J. R. Haas, E. L. Shock, and D. C. Sassani, "Rare earthelements in hydrothermal systems: estimates of standard partial molal thermodynamic properties of aqueous complexes of the rare earth elements at high pressures and temperatures," Geochim. Cosmochim. Acta **59**, 4329–4350 (1995).

L. A. Haskin, "Petrogenetic modeling use of rare earth elements, in *Rare-Earth Element Geochemistry* Ed. by P. Henderson (Elsevier, Amsterdam, 1984), pp. 115–152.

J. L. Heurex and A. D. Fowler, "A non-linear model of oscillatory zoning in plagioclase," Am. Mineral. **79**, 885–891 (1994).

H. Hirai, S. Sueno, and H. Nakazawa, "A lamellar texture with chemical contrast in grandite garnet from Nevada," Am. Mineral. **67**, 1242–1247 (1982).

H. Hirai and H. Nakazawa, "Origin of iridescence in garnet: an optical interference study," Phys. Chem. Mineral. **8**, 25–28 (1982).

H. Hirai and H. Nakazawa, "Grandite garnet from Nevada: confirmation of origin of iridescence by electron microscopy and interpretation of a moire- like texture," Am. Mineral. **71**, 123–126 (1986a).

H. Hirai and H. Nakazawa, "Visualizing low symmetry of a grandite garnet on precession photographs," Am. Mineral. **71**, 1210–1213 (1986b).

T. Holten, B. Jamtveit, P. Meakin, M. Cortini, J. Blundy, and H. Austrheim, "Statistical characterization and origin of oscillatory zoning in crystals," Am. Mineral. **82**, 596–606 (1997).

T. Holten, B. Jamtveit, and P. Meakin, "Noise and oscillatory zoning of minerals," Geochim. Cosmochim. Acta **64**, 1893–1904 (2000).

S. E. Humphris, "The mobility of the rare earth elements in crust," in *Rare-Earth Element Geochemistry* Ed. by P. Henderson (Elsevier, Amsterdam, 1984), pp. 317–342.

S. T. Intayot, Thansasuthipitak, and P. Thansasuthipitak, "The oscillatory zoning in grandite garnet from Khao PhuKha, Lop Buri, Central Thailand," Chiang Mai J. Sci. **34**, 65–71 (2007).

T. I. Ivanova, A. G. Shtukenberg, O. Yu. Punin, O. V. Frank-Kamenetskaya, and P. B. Sokolov, "On the complex zonality in grandite garnets and implications," Mineral. Mag. **62**, 857–868 (1998).

B. Jamtveit, "Oscillatory zonation in hydrothermal grossular andradite garnet: Non-linear dynamics in region of immiscibility," Am. Mineral. **76**, 1319–1327 (1991).

B. Jamtveit and T. Andersen, "Morphological instabilities during rapid growth of metamorphic garnets," Phys. Chem. Mineral. **19**, 176–184 (1992).

B. Jamtveit, R. A. Wogelius, and D. G. Fraser, "Zonation patterns of skarn garnets: records of hydrothermal system evolution," Geology **21**, 113–116 (1993).

B. Jamtveit and R. L. Hervig, "Constraints on transport and kinetics in hydrothermal systems from zoned garnet crystals," Science **263**, 505–508 (1994).

B. Jamtveit, K. V. Ragnarsdottir, and B. J. Wood, "On the origin of zoned grossular–andradite garnets in hydrothermal systems," Eur. J. Mineral. **7**, 1339–1410 (1995).

N. F. Jansson and R. L. Allen, "Timing and setting of skarn and iron oxide formation at the Smältarmossen calcic iron skarn deposit, Bergslagen, Sweden," Miner. Deposita **48**, 313–339 (2013).

Y. Kato, "Rare earth elements as an indicator to origins of skarn deposits: examples of the Kamioka Zn-Pb and Yoshiwara-Sannotake Cu (-Fe) deposits in Japan," Resou. Geol. **49**, 183–198 (1999).

T. A. P. Kwak, W. M. Brown, P. B. Abeysinghe, and T. H. Tan, "Fe solubilities in very saline hydrothermal fluids: their relation tozoning in some ore deposits," Econ. Geol. **81**, 447–465 (1986).

C. G. Lee and W. W. Atkinson, Jr. "Geochemistry of zoned garnets from the San Pedro Mine, Santa Fe County, New Mexico," N. M. Geol. **7**, 69–74 (1985).

P. Lessing and R. P Standish., "Zoned garnet from Crested Butte, Colorado," Am. Mineral. **58**, 840–842 (1973).

Q. Ling and C. Liu, "Geochemical behaviors of REE and other Wace elements during the formation of stratabound skarns and related deposits: a case study of the Dongguashan Cu (Au) Deposit, Anhui Province, China," Acta Geol. Sin. **77**, 246–257 (2003).

Y. G. Liu, M. R. U. Miah, and R. A. Schmitt, "Cerium: a chemical tracer for paleo- oceanic redox conditions," Geochim. Cosmochim. Acta **52**, 1361–1371 (1988).

B. G. Lottermoser, "Rare-earth elements and hydrothermal ore formation processes," Ore Geol. Rev. **7**, 25–41 (1992).

J. S. Marsh, "REE fractionation and Ce anomalies in weathered Karoo doleritie," Chem. Geol. **90**, 189–194 (1991).

H. J Massonne., "Formation of amphibole and clinozoisite- epidote during exhumation of eclogite in a subduction channel," J. Petrol. **53**, 2115–2138 (2012).

A. Masuda, N. Nakamura, and T. Tanaka, "Fine structures of mutually normalized rare-earth patterns of chondrites," Geochim. Cosmochim. Acta **37**, 239–248 (1973).

A. Masuda, "Abundances of monoisotopic REE, consistent with the Leedey chondrite values," Geochem. J. **9**, 183–184 (1975).

A. Masuda and Y. Ikeuchi, "Lanthanide tetrad effect observed in marine environment," Geochem. J. **13**, 19–22 (1979).

E.P. Meagher, "Silicate garnets," in *Orthosilicates,* Ed. by P. H. Ribbe, Rev. Mineral **5**, 25–66 (1982).

L.D. Meinert, "Skarns and skarn deposits," Geosci. Can. **19**,145–162 (1992).

L. D. Meinert, "Application of skarn deposit zonation models to mineral exploration," Explor. Min. Geol. **6**, 185–208 (1997).

G. Mongelli, "REE and other trace elements in a granitic weathering profile from "Serre", Southern Italy," Chem. Geol. **103**, 17–25 (1993).

E. Murad, "Zoned, birefringent garnets from Thera Island, Santorini Group (Aegean Sea)," Mineral. Mag. **40**, 715–971 (1976).

T. Nakano, H. Takahara, and N. Norimasa, "Intracrystalline distribution of major elements in zoned garnet from skarn in the Chichibu mine, central Japan; illustration by color-coded maps," Can. Mineral. **27**, 499–507 (1989).

H. W. Nesbitt, "Mobility and fractionation of rare-earth elements during weathering of a granodiorite," Nature **279**, 206–210 (1979).

P. Ortoleva, E. Merino, C. Moore, and J. Chadam, "Geochemical self-organization 1: Reaction-transport feedback sand modeling approach," Am. J. Sci. **287**,979–1007 (1987).

J. M. Parr, "Rare-earth element distribution in exhalites associated with Broken Hill-type mineralization at the Pinnacles deposit, New South Wales, Australia," Chem. Geol. **100**, 73–91 (1992).

Y. Perfiliev, L. Aistov, and E. Selivanov, "Geology and minerals of Khur area (central Iran), Report 3," (V/O Technoexport, Moscow, 1979).

D. Z. Piper, "Rare earth elements in the sedimentary cycle: a summary," Chem. Geol. **14**, 285–304 (1974).

M. I. Prudencio, M. S. A. Braga, and M. A. Gouveia, "REE mobilization, fractionation and precipitation during weathering of basalts," Chem. Geol. **107**, 251–254 (1993).

R. D. Shannon, "Revised effective ionic radii and systematic studies of interatomic distance in halides and chalcogenides," Acta Crystall. (A) **32**, 751–767 (1976).

M. Shore and A. D. Fowler, "Oscillatory zoning in minerals: a common phenomenon," Can. Mineral. **34**, 1111–1126 (1996).

M. P. Smith, P. Henderson, T. E. R. Jeffries, J. Long, and C. T. Williams, "The rare earth elements and uranium in garnets from the Beinn and Dubhaich Aureole, Skye, Scotland, UK: constraints on processes in a dynamic hydrothermal system," J. Petrol. **45**, 457–484 (2004).

F. S. Spear, "Metamorphic Phase Equilibria and Pressure–Temperature–Time Paths," (Mineralogical Society of America, Washington, D.C, 1993).

B. E. Taylor and J. R. O'Neil, "Stable isotope studies of metasomatic Ca-Fe-Al-Si skarns and associated metamorphic and igneous rocks, Osgood Mountains, Nevada," Contrib. Mineral. Petrol. **63**, 1–49 (1977).

B. E. Taylor and J. G. Liou, "The low-temperature stability of andradite in C–O–H fluids," Am. Mineral. **63**, 378–393 (1978).

R. P. Taylor and B. J. Fryer, "Multi-stage hydrothermal alteration in porpphyry copper systems in northern Turkey: the temporal interplay of potassic, porphylitie and phyllic fluids," Can. J. Earth Sci. **17**, 901–926 (1980).

R.P. Taylor and B.J. Fryer, "Rare earth element geochemistry as an aid to interpreting hydrothermal ore deposits," in *Metallization Associated with Acid Magmatism,* Ed. by A. M. Evans (Wiley, New York, 1982), pp. 357–365.

C. H. Van der Weijden, and R. D. Van der Weijden, "Mobility of major, minor and some redox-sensitive trace elements and rare earth elements during weathering of four granitoids in central Portugal," Chem. Geol. **125**, 149–168 (1995).

D. J. Whifford, M. L. Korsch, P. M. Porritt, and S. J. Craven, "Rare-earth element mobility around the volcanogenic polymetallic massive sulfide deposit at Que River, Tasmania, Australia," Chem. Geol. **68**, 105–119 (1988).

P. R. Whitney and J. F. Olmsted, "Rare earth element metasomatism in hydrothermal systems: the Willsboro-Lewis wollastonite ores, New York, USA," Geochim. Cosmochim. Acta **62**, 2965–2977 (1998).

D. L. Whitney and B. W. Evans, "Abbreviations for names of rock forming minerals," Am. Mineral. **95** (1), 185–187 (2010).

S. A. Wood, "The aqueous geochemistry of the rare-earth elements and yttrium. 2. Theoretical predictions of speciation in hydrothermal solutions to 350°C at saturation water vapor pressure," Chem. Geol. **88**, 99–125 (1990).

S. A. Wood and A. E. Williams-Jones, "The aqueous geochemistry of the rare-earth elements and yttrium. 4. Monazite solubility and REE mobility in exhalative massive sulfide-depositing environments," Chem. Geol. **115**, 47–60 (1994).

B. W. D. Yardley, C. A. Rochelle, A. C. Barnicoat, and G. E. Lioyd, "Oscillatory zoning in metamorphic minerals: an indicator of infiltration metasomatism," Mineral. Mag. **55**, 357–365 (1991).

V. Yakovenko, I. Chinakov, Yu. Kokorin, and B. Krivyakin, "*Report on Geological Prospecting in Anarak Area (Kal-e Kafi- Khuni Locality)*," (V/O Technoexport, Moscow, 1981), No. 13.

Z. Zhang and S. K. Saxena, "Thermodynamic properties of andradite and application to skarn with coexisting andradite and hedenbergite," Contrib. Mineral. Petrol. **107**, 255–263 (1991).